

A Novel Particle Morphological Investigation of Mineral Ore Particles by A Morphologically Directed Raman Spectroscopy

SASAKURA, Daisuke^{1*} ; HAMADA, Hiroyuki¹ ; HAYAUCHI, Aiko¹

¹Malvern Instruments, A division of Spectris Co., Ltd.

[Introduction]

To investigate of the mineral resources as particles such as soil in sea, in ground and in fields is interesting in geochemistry. The existing approach to investigate of mineral resources, the manual microscopic observation method and an elemental analysis technics had been used. The major drawback of a manual microscope approach has been used for few number of particles morphology observation. It is not able to described particle shape as significant number. Furthermore an elemental analysis technique such as X-Ray fluorescence and destructive wet chemical analysis can determine the quantity of mineral species present in the ore, however, these chemical analysis methods do not allow the study of the composition of individual particles of different size and shape. The morphologically directed Raman spectroscopic (MDRS) is a novel approach which can resolve this problem. Using this method the Raman spectra of several hundred particles is determined after size and shape classification of each individual particle by automated particle image analysis. Raman spectroscopy can be used to acquire the spectra of any inorganic compounds such as metal oxides and nitrides which are Raman active. Many mineral resources are mined as inorganic compounds. Therefore, Raman spectroscopy can be used for the identification of the chemical composition of mineral ores. Using the a morphologically directed Raman spectroscopic method described herein, it is possible to calculate the particle size distribution and proportion by mass or volume of each chemical component or mineral species based on Raman spectroscopic information. This study will report and discuss the capability MDRS method using a model material.

[Material and Method]

These samples had been through the ore dressing process. MDRS measurement was carried out using a Morphologi G3SE-ID instrument (Malvern Instruments, UK) equipped with a dry powder sample dispersion unit (SDU) and Raman module. The laser wavelength of Raman excitation was 785nm the laser power was less than 5mW and the irradiation time was 5 sec. The particle image measurements were made in diascopic mode with a total magnification 250x. Iron ore dry powder samples were dispersed using the SDU using a short duration pulse of compressed air. Measurements were made automatically using Standard Operating Procedures (SOPs) which define the software and hardware settings used. Measurement sample was dispersed on to glass plate as sample carrier which was minimized environmental exposure by the enclosed sample chamber unit. Particle identification by Raman analysis used the spectrum correlation coefficient approach.

Keywords: Particle Size, Particle Shape, Morphology, Raman, Resource analysis

Raman spectroscopic analysis of carbonaceous material included in oil source rocks

KOUKETSU, Yui^{1*} ; OKUMURA, Fumiaki² ; IWANO, Hirotsugu² ; WASEDA, Amane² ; KAGI, Hiroyuki¹

¹Geochemical research center, Graduate School of Science, The University of Tokyo, ²Japan Petroleum Exploration Co.,Ltd. (JAPEX)

Carbonaceous material (CM) included in rocks is important material to produce resources of oil and gas. The quality and storage of these resources are evaluated by analyzing the chemical composition, crystal structure, and reflectance of CM. In the oil exploration, vitrinite reflectance is widely used to evaluate the maturity of CM. However, the spatial resolution of vitrinite reflectance measurement is about 10 μm and more than 100 point measurement is needed for quantitative evaluation. Therefore, the evaluation of maturity of CM is sometimes difficult in low vitrinite content rocks.

In the present study, we examined the maturity of CM using the Raman spectroscopy, whose spatial resolution is about 1 μm . Kouketsu et al. (2014, Island Arc) reported that the values of full width at half maximum (FWHM) of CM Raman spectra correlate with metamorphic temperature and proposed the Raman CM geothermometer. Applicable temperature range is 150 to 400 $^{\circ}\text{C}$ and the reflectance of vitrinite included in the calibrated samples is more than 1 %. We focused on the reflectance less than 1 % where the crude oil is started to produce and carried out the measurement of Raman spectroscopic analysis and reflectance for the samples containing vitrinite grains whose reflectance between 0.25 to 2.44 %.

In the Raman spectroscopic analysis, we used 514.5 nm Ar^{+} laser and set the laser power around 0.2 mW at sample surface to avoid the damage to CM. Measured spectra were divided into four peaks of D1-, D2-, D3-, and D4-bands within the 1000 to 2000 cm^{-1} range. Raman spectra of CM less than 1 % of reflectance show strong fluorescence background. Raman peaks of CM less than 0.4 % of reflectance cannot be detected. The values of FWHM of D1- and D2-bands vary less than 1 % of reflectance range and the correlation becomes unclear. The CM Raman spectra seem to be affected by the background and peaks are not separated properly. This result indicates that the conventional Raman CM geothermometer is difficult to apply to oil source rocks. On the other hand, the slope of Raman baseline becomes smaller with increasing reflectance, and the correlation is approximated by exponential function. The fluorescence related to the baseline of Raman spectra is considered to be caused by the polycyclic aromatic hydrocarbon that is the main component of oil and gas. Therefore, the baseline slope of CM Raman spectra will be a useful index to evaluate the maturity of oil source rocks.

Keywords: oil source rock, carbonaceous material, Raman spectroscopy, vitrinite reflectance

Petrological and spacial variations of the near off-axis magmatism controlled by a ridge segment structure

KANEKO, Ryu^{1*} ; ADACHI, Yoshiko¹ ; MIYASHITA, Sumio¹

¹Niigata University

It is thought that the ridge segment structure controls partial melting proceses of upper mantle and supply system of magmas at the mid-ocean ridges (MacDonald et al., 1988), and we may observe these occurrences at the Oman ophiolite. Fizeh and Salahi blocks of the northern Oman ophiolite is corresponded to the 2nd order ridge segment (Adachi and Miyashita, 2003; Miyashita et al., 2003), wehrlitic intrusions of the near off-axis magmatism are identified different petrological features. The presence of magmatic hornblende is rare in the segment centre but more abundant of hornblende and orthopyroxene at the segment margin (Adachi and Miyashita, 2003; Kaneko et al., 2014). The forsterite content of olivine and the Mg# of clinopyroxene from the wehrlitic intrusions of the segment margin are more evolved than in rocks from the segment centre. Chlorine contents of magmatic hornblende from the segment centre and margin show high contents.

Although Phyton et al. (2007) identified that the seawater penetrates the lower oceanic crust, this study suggests the fluid of seawater implicates magma compositions of near off-axis magmatism. We focus on vertical variations of wehrlitic intrusions, and show the spatial variation of petrographic features and mineral compositions in the along ridge axis, and then perform a three-dimensional study of hydrothermal circulation along the ridge segment structure. It is important to elucidate of the seawater penetrating depth at the oceanic crust formation, we discuss the change in the penetration depth of the seawater along axis, trying to understand of the oceanic crust formation process.

Keywords: near off-axis magmatism, ridge segment structure, wehrlitic intrusion, Oman ophiolite

Mineralogical characterization of groundmass nanolites in the Shinmoedake 2011 eruption products

MUJIN, Mayumi^{1*}; NAKAMURA, Michihiko¹; MIYAKE, Akira²

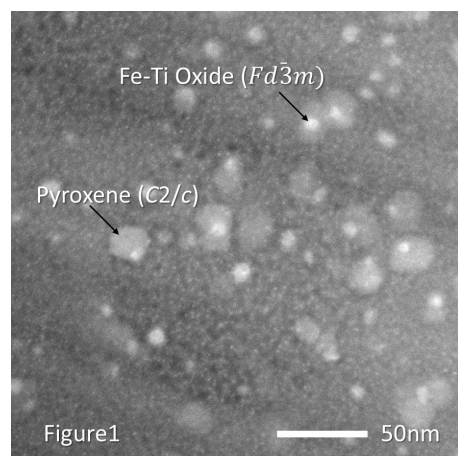
¹Department of Earth and Planetary Material Science, Graduate School of Science, Tohoku University, ²Division of Earth and Planetary Sciences, Graduate School of Science, Kyoto University

The groundmass nanolites are submicron scale minerals having a steeper slope of CSD (crystal size distribution) than microlites, originally described for a rhyolitic dome lava (Ben Lomond rhyolite lava dome; Sharp et al., 1996). The nanolites in explosive eruption products were first reported by Mujin and Nakamura (2014) for the pumices and dense juvenile fragments of the Shinmoedake (Kirishima Volcano) eruption in 2011. They found that the mineral assemblage of the nanolites recorded eruption style transition from sub-Plinian pumice, via Vulcanian pumice to lava cap as follows: pyroxene (pyx), pyx + plagioclase (pl), and pyx + pl + Fe-Ti oxides in a descending order of explosivity. In this study, we report their chemical compositions and crystal space groups.

The fine plagioclase microlites in the sub-Plinian pumices have clearly higher An contents (by ca. 5 mol%) than the similarly sized plagioclase (mostly nanolites) in the Vulcanian pumices and lithic fragments. This indicates that the pumices of Sub-Plinian eruption quenched before nanolite nucleation and growth of fine microlite ($<3 \mu\text{m}$ in width). The decrease in An content from the microlites to the nanolites may be explained by considering two factors: 1) crystallization differentiation of the melt, and 2) decompression and possibly cooling during crystallization.

The compositions of pyroxene nanolites and small microlites ($1 - 6 \mu\text{m}$ in width), on the other hand, do not show any systematic difference among the eruption styles, being consistent with the CSD results. They were within the metastable compositional range of pigeonite, sub-calcic augite and augite. In the electron diffraction pattern of TEM, we identified the pyroxenes and Fe-Ti oxide crystals as small of 20 and 10 nm in the dense juvenile fragments, respectively. In the HAADF-STEM images (Fig. 1), the pyroxene and Fe-Ti oxide crystals as small as 3 and 1 nm were discernable. Some Fe-Ti oxide crystals were formed on the pyroxene crystal surfaces, suggesting that some of the crystals nucleated heterogeneously. The crystal systems of pyroxene and Fe-Ti oxide nanolites were determined as $C2/c$ and $Fd-3m$, respectively. This is in contrast to the previously reported pyroxene nanolites in the lava dome sample (Sharp et al., 1996). They were composed of the mixture of orthopyroxene and clinopyroxene, and a complex micro-structure resulting from sub-solidus exsolution from pigeonite ($P2_1/c$) to augite ($C2/c$) and hypersthene. Sharp et al. (1996) interpreted this complexity of pyroxene phases resulted from moderate cooling rate within the obsidian layer. By contrast, we did not confirm the subsistent of the mixed pyroxenes in dense fragments of the Shinmoedake eruption products, because the scale of the observed pyroxene was 1 - 2 orders of magnitude smaller than that of Sharp et al. (1996). The appearance of a metastable phase of pyroxene nanolites and fine nanolites ($1 - 20 \text{ nm}$) in the dense fragments seems to be resulted from the nucleation and growth under large super cooling followed by rapid quenching. The large undercooling may have been produced though rapid magma ascent and succeeding dehydration and liquidus increase, in addition to the cooling and oxidation of the magma near the surface.

Keywords: Nanolite, undercooling, TEM, pyroxene, Fe-Tioxide, plagioclase



Zircon U-Pb ages of Early Crataceous igneous rocks in the Kitakami Mountains, Japan

TSUCHIYA, Nobutaka^{1*} ; SASAKI, Jun¹ ; ADACHI, Tatsuro² ; NAKANO, Nobuhiko² ; OSANAI, Yasuhito²

¹Iwate University, ²Kyushu University

Early Cretaceous igneous rocks in the Kitakami Mountains consist of volcanic rocks, dike rocks, and plutonic rocks, from older to younger. Plutonic rocks are composed mainly of adakitic granites in central part of zoned plutonic bodies surrounded by adakitic to non-adakitic granites in marginal part. These adakitic plutons is divided into E and W zones based on the ages and geochemistry. Zircon U-Pb ages were determined with laser ablation inductively coupled plasma mass spectrometry (LA-ICP-MS) for 22 samples from 13 rock bodies including the Early Cretaceous adakitic granites in the Kitakami Mountains (Tsuchiya et al., 2015). Zircons from the adakitic granites of E zone give older ages (127–117 Ma) compared with those of W zone (119–113 Ma). Zircon ages become younger from the northern Hashikami pluton and marginal facies of the Tanohata pluton (127–125 Ma) to southern Takase granites (118–117 Ma), in the E zone adakitic granites. Petrochemical differences between the E zone and W zone rocks indicate that the adakitic melt of E zone rocks are considered to be derived from vapor-absent melting condition, while those of W zone rocks are from higher pressure and vapor-present condition. Calc-alkaline to shoshonitic plutonic rocks and dike rocks show narrow range of zircon U-Pb age (128–124 Ma), and are almost contemporaneous to those of the Hashikami, Tanohata, and Miyako plutons (127–125 Ma). Taking all these data into consideration, the Early Cretaceous magmatism in Kitakami can be explained by the differential subduction model of the Farallon-Izanagi plates or slab rollback model accompanied with asthenospheric upwelling.

Keywords: adakite, zircon geochronology, Kitakami, petrochemistry, Cretaceous

Rock facies of The Hikami granitic body in south Kitakami Mountains, Japan

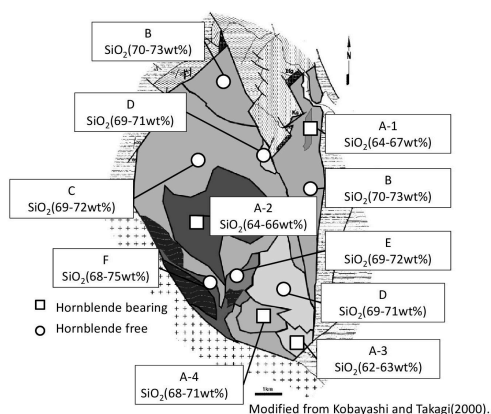
SASAKI, Jun^{1*} ; TSUCHIYA, Nobutaka¹

¹Iwate University

The Hikami Granitic Rocks, one of the oldest granites in Japan, crops out from central to eastern part of the South Kitakami Belt. The Hikami Granitic Rocks are distributed mainly around Mt. Hikami, and northern part of small masses. The Hikami Granitic Rocks has long been controversial on their age of intrusion. Sasaki et al. (2013, 2014) examined the zircon U-Pb ages of 13 samples from the Hikami Granitic Rocks, and solidification age of around 450 Ma were obtained.

The Hikami Granitic Rocks were subdivided lithologically into nine types, A-1, A-2, A-3, A-4, B, C, D, E and F on the basis of Asakawa et al. (1999), Kobayashi and Takagi (2000). Petrochemical characteristics of major and minor elements indicate that the Hikami Granitic Rocks are derived from fractional crystallization through a common parental magma.

Keywords: Hikami Granitic Rocks, Petrochemistry, south Kitakami Mountains, Pre-Silurian



Crystalized melt inclusions in mafic granulite: investigation of partial melting process based on pseudosection

SAITOH, Yohsuke^{1*}; TSUNOGAE, Toshiaki¹

¹Yohsuke Saitoh

We report here new petrological date of crystalized melt inclusions (CMIs) and phase equilibrium modeling of partially melted mafic granulite to evaluate the influence of partial melting to the phase relation from the Neoproterozoic - Cambrian Lutzow-Holm Complex (LHC), East Antarctica (Shiraishi et al., 1992). Previous petrological studies of the LHC suggest an increase in the metamorphic grade from northeast (amphibolite facies) to southwest (granulite facies) (Hiroi et al., 1991). CMIs are often reported from the pelitic and felsic granulites (e.g. Cesare et al., 2009). However they are relatively rare in mafic to ultramafic granulites. We thus attempt to investigate textures of the CMIs in the mafic to ultramafic granulites to discuss the partial melting process.

The examined mafic and ultramafic granulites occur as boudin or small blocks of several meters within psammitic and hornblende-biotite gneisses of the granulite-facies zone. Based on detailed microscopic observations, we found CMIs bearing mafic and ultramafic granulites from four different exposures within the LHC. The representative samples of mafic to ultramafic granulite are composed mainly of coarse-grained garnet, hornblende, orthopyroxene, clinopyroxene, plagioclase, and ilmenite. The garnet often contains CMIs. The CMIs consist of fine-grained quartz, orthopyroxene, biotite, K-feldspar, plagioclase, and ilmenite which size varies from 1 to 50 μ m. The size of CMI grains is up to 100 μ m, and they show negative crystal shapes of the host garnet. We subsequently calculated chemistry of the CMIs based on modal abundance and chemistry of the minerals for each CMI. The results are nearly equivalent to the compositions of andesitic to dacitic melt.

Occurrence of hornblende and biotite within garnet in the rock suggests dehydration melting of the hydrous minerals and formation of andesitic to dacitic melt during prograde stage. Phase equilibrium modeling in NCKFMASHTO system demonstrated that some mafic to ultramafic granulites experienced considerable amounts of melt loss (up to 6.5-7 wt. %) defined by the stability field of clinopyroxene and modal isopleth of clinopyroxene. Stability field of quartz expands toward lower pressure side with increase of melt amount in the phase diagram. Based on phase equilibrium modeling of melt-bulk interaction, the stability field of quartz and clinopyroxene is critical to estimate the P-T condition and amounts of melt extraction during partial melting. We estimated peak P-T condition of 900 °C and 10-11 kbar and clockwise P-T path for the rock based on the integrated bulk composition. Modal isopleth of the mineral also demonstrated that partial melting progressed through the following reactions. $Hbl + Bt \rightarrow Liq + Cpx + Grt$. $Hbl + Pl \rightarrow Liq + Cpx + Grt$. This study demonstrated that partial melting took place under plagioclase free field and plagioclase stable field.

The peak condition is comparable with previous estimations of 800-950 °C and 7-12 kbar (Yoshimura et al., 2004). Our results suggest that partial melting and melt loss are common processes even in mafic to ultramafic granulites from the LHC, and CMIs could preserve the composition of melt which has already been extracted from the system. Phase equilibrium modeling suggests that melt loss during prograde stage have critical influence on the mineral assemblage and stability field of the mineral of the examined samples.

References

- Cesare, B., Ferreol, S., Salvioli, M.E., Pedron, D., Cacallo, A., 2009. *Geology* 37, 627-630.
- Hiroi, Y., Shiraishi, K., Motoyoshi, Y., 1991. *Geological Evolution of Antarctica*, Cambridge University Press, Cambridge, 83-87.
- Shiraishi, K., Hiroi, Y., Ellis, D.J., Fanning, C.M., Motoyoshi, Y., Nakai, Y., 1992. *Recent Progress in Antarctic Earth Science*. Terra, Tokyo, 67-73.
- Yoshimura, Y., Motoyoshi, Y., Miyamoto, T., Grew, S. Edward., Carson, J. Christopher., Dunkley, J. Daniel., 2004. *Polar Geoscience* 17, 57-87.

Keywords: crystalized melt inclusions, mafic granulite, Lutzow-Holm Complex, phase equilibrium modeling

Chemical Modification of Felsic Melt by Reaction with Peridotite: Implications from the Magarisawa Peridotite, Hokkaido

YAMASHITA, Kohei^{1*}; MAEDA, Jinichiro²; YOSHIKAWA, Masako³; SHIBATA, Tomoyuki³; YI, Keewook⁴

¹Department of Natural History Sciences, Graduate School of Science, Hokkaido University, ²Department of Natural History Sciences, Faculty of Science, Hokkaido University, ³Beppu Geothermal Research Laboratory, Kyoto University, ⁴Geochronology Team, Korea Basic Science Institute

It has been well-documented that subduction zone magmatism is induced by partial melting of the hydrated wedge mantle (e.g., Sakuyama, 1982) and/or of subducting slab (e.g., Wyllie and Sekine, 1982). In the latter case, felsic partial melts would have to undergo interaction with peridotites during upward migration through the overriding wedge mantle (e.g., Kay, 1978). However, the detail of felsic melt/peridotite interaction processes has not been fully described due to very rare natural occurrence suitable for petrological examinations (e.g., Shimizu et al., 2004).

We found felsic veins of various size (microscopic order to ca. 50 – 60 cm in width) and with a wide compositional range in the Magarisawa Peridotite (MP), northern Hidaka Mountains, Hokkaido. The MP, one of the mantle peridotite masses situated along the base of the Hidaka Magmatic Belt (Maeda et al., 1986), is mainly composed of Pl lherzolite, and surrounded by pelitic granulites and their anatectic equivalents. Here we present zircon SHRIMP U-Pb age, major element compositions, and ⁸⁷Sr/⁸⁶Sr and ¹⁴³Nd/¹⁴⁴Nd isotopic ratios of felsic veins, in order to discuss the chemical modification process of the felsic melts by interaction with mantle peridotite observed in the MP.

On the basis of lithology and whole-rock compositions of the felsic veins, we subdivided them into three facies: (1) Granitic Vein (GV; Qz + Kfs + Pl + Phl + Opx ± Cpx ± Zr ± Ap ± Rtl ± Sph), characterized by higher-SiO₂ (64.0 – 74.5 wt%) and -K₂O (2.1 – 5.8 wt%), and lower-MgO (0.4 – 2.1 wt%) contents, (2) Pl-veinlet (PV; Plagioclase ± Opx ± Kfs ± Phl ± Zr ± Ap), which is a thin veinlet branched from the GV, (3) Noritic Vein (NV; Pl + Opx ± Phl ± Zr ± Ap ± Fe-Ni sulfide ± Ox), characterized by lower-SiO₂ (55.0 – 60.0 wt%) and -K₂O (<0.8 wt%), and higher-MgO (2.3 – 6.5 wt%) contents. Although continuous transition between the GV and the NV has not been observed in the field until now, whole-rock composition of the both veins represent a single trend on the Harker diagram. The PV is intermediate on the trend between the GV and the NV.

Orthopyroxenite (0.5 – 1.5 mm in thickness) composed of mosaic-shaped secondary Opx with subordinate amounts of Phl is always observed along the vein/peridotite boundary, clearly suggesting that the veins were formed from SiO₂-oversaturated melts and reacted with Ol in peridotites (e.g., Sen and Dunn, 1994). Furthermore, the microscopic/microprobe analyses indicate that secondary Opx is also formed by reaction between the felsic melts and primary Opx, Cpx, and Spl in the host lherzolite.

Zircon U-Pb age of the Noritic Vein is 19.5 ± 0.25 Ma, which corresponds to one of the main phases of the Hidaka magmatism and metamorphism (e.g., Maeda et al., 2010).

⁸⁷Sr/⁸⁶Sr initial ratios of GV, PV and NV are 0.70531 – 0.70550, 0.70541 – 0.70551 and 0.70560 – 0.70566, respectively, and ¹⁴³Nd/¹⁴⁴Nd initial ratios of them are 0.51258 – 0.51260, 0.51260 – 0.51261, 0.51245 – 0.51260, respectively. Isotopic compositions of all felsic veins are apparently similar to those of the pelitic granulite/anatexite surrounding the MP (Maeda and Kagami, 1996).

Because formation of Opx from Ol consumes SiO₂ in the melts, the successive melt should become less-silicic, indicating the continuous modification of the melt composition from the GV through the PV to the NV. We have performed simple mass balance calculations to derive the NV from GV for major element composition. The results show that the composition of the NV can be modeled by addition of Ol, Cpx and Spl (in the host peridotite) to and subtraction of Opx and Phl (in the orthopyroxenite) from the GV.

In summary, we propose that the felsic veins within the MP record a significant chemical modification of SiO₂-oversaturated felsic melt during the interaction with mantle peridotite.

Characteristics of chromitites from the Higashi-akaishi ultramafic complex: Implications for origin of UHP chromitite

MIURA, Makoto^{1*} ; ARAI, Shoji¹ ; MIZUKAMI, Tomoyuki¹ ; YAMAMOTO, Shinji² ; VLADIMIR, Shmelev³

¹Department of Earth Sciences, Kanazawa University, ²Department of Earth Science and Astronomy, University of Tokyo, ³Institute of Geology and Geochemistry, Ural Branch Russian Academy of Sciences

Ultrahigh-pressure (=UHP) chromitites, which contain UHP minerals such as diamond and coesite, have been observed from ophiolites in Tibet and the Polar Urals. However, their nature, i.e. origin, frequency of appearance and P-T path, are still controversial because of insufficiency of detailed petrographic studies. Systematic observation and classification of various chromitites and enclosing peridotites from some localities are required.

Chromitites in the Higashi-akaishi ultramafic complex in the Cretaceous Sanbagawa metamorphic belt, Japan, is one of keys to interpret the origin of UHP chromitite. The Higashi-akaishi ultramafic complex is characterized by the presence of garnet in some peridotites and pyroxenites, and interpreted as a high-P metamorphic (up to 3.8 GPa) complex originally formed at a lower-P subduction zone mantle. The chromitites in the Higashi-akaishi ultramafic complex had also experienced the high-P metamorphism. They will provide us with information on the behavior of low-P chromitite upon compression via subduction.

Spinel in the Higashi-akaishi chromitite contains various inclusions, i.e. numerous needle- and blade-like diopside lamellae, and is free of primary inclusions of hydrous minerals, such as pargasite and Na phlogopite. Solid-phase secondary inclusions are mostly composed of chlorite and serpentine. Chromian spinels in the Higashi-akaishi chromitite show high Cr#s (0.8 to 0.85) and low Ti contents (<0.1 wt%), suggesting an arc-related feature. Spinel in the Higashi-akaishi chromitite and surrounding peridotite were sometimes fractured by deformation.

The Higashi-akaishi chromitite is similar in features of inclusions in spinel and spinel chemistry to the UHP chromitites from Tibet and the Polar Urals. This similarity suggests that some of the characteristics of the UHP chromitite can be formed by compression of low-P chromitite, e.g., recycling via a subduction zone. In addition, such diopside lamellae in spinel of the Higashi-akaishi chromitite are typically found from some low-P chromitites from the Oman ophiolite and the Iwanai-dake ultramafic complex, Japan. Their occurrence suggests that the UHP Ca-ferrite (or Ca-titanite) type spinel precursor is not a prerequisite for exsolution of silicate lamellae.

Keywords: Podiform chromitite, The Higashi-akaishi ultramafic complex, Spinel, Exsolution lamella, Ultrahigh-pressure chromitite

Phase transition of sillimanite with Al/Si-disordering at high temperature

IGAMI, Yohei^{1*}; KOGISO, Tetsu²; OHI, Shugo¹; MIYAKE, Akira¹

¹Kyoto Univ., Sci., ²Kyoto Univ., HES.

Naturally occurring polymorphs of Al_2SiO_5 (andalusite, kyanite, sillimanite) have assumed a special significance for geologists because of their value as indicators of the pressures (P) and temperatures (T) experienced by metamorphic rocks. Especially, sillimanite may have more geological information in its crystal structure or microstructure. For example, it has been indicated experimentally that sillimanite show the structures like anti-phase boundaries (APB) and/or enrich to Al releasing SiO_2 -rich melt at high temperature (Holland & Carpenter, 1986). Miyake et al. (2008) showed sillimanite in Napier complex has APB-like structure and fine mullite inclusion (which is more Al-rich than sillimanite, $\text{Al}_2[\text{Al}_{2+2x}\text{Si}_{2-2x}\text{O}_{10-x}]$). In addition, Greenwood (1972) suggested the phase of completely Al/Si-disordered sillimanite as another phase from sillimanite. And, Fischer et al. (2014) found new phase different from sillimanite, mullite, and “completely Al/Si-disordered sillimanite”. These phase also can be valuable geological indicator, but their behaviors are not clear. They need very high resolution for analysis to be detected and classified. Like this, phase relation of sillimanite at high T (and high P) is still so confused. In this study, synchrotron powder X-ray diffraction (XRD) and transmission electron microscope (TEM) experiments were carried out on samples of sillimanite heat-treated in various conditions (P , T and duration time) in order to clarify behavior of sillimanite at high temperature.

We heated sillimanite ($\text{Al}_{2.00}\text{Si}_{0.99}\text{Fe}_{0.01}\text{O}_5$) crystals in Rundvagshetta, Lutzow-Holm, Antarctica.sillimanite in the range of 0.8-2.5GPa, 1000-1500 °C for 10-1751 hours and then quenched. Experimental products (46 samples) were examined by Synchrotron powder XRD experiment at BL-4B₂ in photon factory, KEK and observed TEM (JEOL JEM-2100F) from the viewpoint of l -odd reflections (which distinct with Al/Si-disordering) and chemical composition.

As a result of XRD experiments, the diffraction patterns of mullite were observed in many samples. Moreover, in four samples heated at 1300-1400 °C, 1GPa, the peaks of unknown phase were observed in addition to that of sillimanite and mullite. This phase have an intermediate feature between peaks of sillimanite and mullite. (So, we will call it “intermediate-phase” .) As a result of TEM observation of these four samples, grains of the intermediate-phase did not give $l = \text{odd}$ reflections, which are characteristic of sillimanite, but distinct with Al/Si-disordering. By chemical analysis (TEM-EDS), the intermediate-phase was slightly Al-rich more than sillimanite but less than mullite. So, It was revealed that the intermediate-phase has the structure which has disordered distribution of Al/Si on the tetrahedral sites, with releasing very little SiO_2 from Al_2SiO_5 . This phase can be stable at high temperature and 1GPa. The intermediate-phase is probably not same as “completely Al/Si-disordered sillimanite” by Greenwood (1972) etc., but may be same as the new phase founded by Fischer et al. (2014). The sillimanite with APB and fine mullite inclusion by Miyake et al. (2008) can be explained as that sillimanite transformed from intermediate phase with mullite. APB was made by Al/Si-ordering when intermediate phase transformed to sillimanite.

References:

- [1]Holland & Carpenter (1986) Nature, 320, 151-153
- [2]Miyake et al. (2008) JAMS Annual Meeting Abstract
- [3]Greenwood (1972) THE Geological Society of America, 132, 553-571
- [4]Fischer et al. (2014) IMA General Meeting Abstract, 21, 335

Keywords: sillimanite, mullite, Al/Si-disordering, synchrotron X-ray experiment

Size effect on the phase transition between protoenstatite and clinoenstatite

OSAKO, Tatsuya^{1*}; OHI, Shugo¹; IGAMI, Yohei¹; MIYAKE, Akira¹

¹Kyoto Univ. Sci.

[Introduction]

Protoenstatite(PEN, space groupe:*Pbcn*), one of the polymorph of enstatite(MgSiO_3), is the stable phase at high temperature above 1000 °C below 1557 °C at atmospheric pressure. It is generally known that protoenstatite is the unquenchable phase. Actually, PEN has never been reported from natural specimens to date. However, Foster (1951), Lee and Heuer(1987), and so on reported PEN was observed at room temperature from experimental generative materials.

Smyth(1974) studied in detail the transformations among polymorphs of enstatite using high temperature single-crystal X-ray techniques. He showed that in rapid quench PEN transformed to clinoenstatite(CEN, $P2_1/c$) and in slow cooling rate PEN transformed to orthoenstatite(OEN, *Pbca*), and concluded that the rapid transformation between PEN and CEN occurs martensitically. On the martensitic transformation, in general, it is known that the transformation starting temperature is effected by the grain size that is i.e. the smaller grain has the lower starting temperature.

It is inferred that grain size affect the PEN-to-CEN transformation because the transformation is considered martensitic. The purpose of this study is to make clear the condition PEN can retain at room temperature which associated with grain size.

[Experiments]

The starting material of experiments was OEN synthesized by the flux method according to Ozima(1982). We crushed and as-sorted synthetic OEN as grain size ($\sim 3\mu\text{m}$, $\sim 10\mu\text{m}$, $35\sim 51\mu\text{m}$, $32\sim 63\mu\text{m}$, $51\sim 73\mu\text{m}$, $73\sim 96\mu\text{m}$, $63\sim 125\mu\text{m}$, $96\sim 105\mu\text{m}$), and heated these samples by the box electric furnace at 1200 °C for 20 hours, and after that cooling rate was 5 °C/min. And furthermore at the synchrotron radiation institution Photon Factory we examined the in situ observation of the PEN to CEN transformation at high temperature to obtain the transformation starting temperature.

[Results]

Only CEN peaks existed in the larger sample than $73\sim 96\mu\text{m}$, on the other hand both CEN and PEN peaks existed in the smaller than $51\sim 73\mu\text{m}$. In $73\sim 96\mu\text{m}$ sample the PEN to CEN transformation started at about 700 °C, however in the $\sim 3\mu\text{m}$ sample the transformation started at about 600 °C. These results indicate that the grain size evidently affect the phase transition temperature between PEN and CEN, that is, the PEN-to-CEN transformation is martensitic. Furthermore these suggest that PEN can retain at room temperature if its size is on the order of several $10\mu\text{m}$ and less.

[1]Foster(1951), *J. Am. Ceram. Soc.* 34 [9], 255-259.

[2]Lee end Heuer(1987), *J. Am. Ceram. Soc.* 70 [5], 349-360.

[3]Ozima(1982), *Ganseki Koubutsu Kousyogaku Gakkaishi Tokubetsugo*(Japanese) 3, 97-103.

Keywords: enstatite, phase transition, size effect

Mineral chemistry of anorthite megacryst and its inclusions from Mt. Fubo, Minami Zao

ECHIGO, Takuya^{1*}; NISHIMAKI, Shino²; TANIGUCHI, Naoki¹; KIMATA, Mitsuyoshi³; SHIMIZU, Masahiro³; SAITO, Shizuo⁴; NISHIDA, Norimasa⁵

¹Faculty of Education, Shiga University, ²Master's Program in Science and Engineering, University of Tsukuba, ³Doctoral Program in Earth Evolution Sciences, University of Tsukuba, ⁴Institute of Materials Science, University of Tsukuba, ⁵Research Facility Center for Science and Technology, University of Tsukuba

Anorthite megacrysts, which are high-calcic plagioclase (An >90 mol%) phenocrysts larger than 10 mm, are characteristic minerals occurring in basalt - andesite from Japanese Islands arc (Kimata et al. 1995). Anorthite megacrysts from Miyakejima contains various inclusions such as native copper (Cu: Murakami et al. 1991), native zinc (Zn: Nishida et al. 1993) and native brass (Zn-Cu alloy: Nishida et al. 1993). In addition, hydrocarbon was also reported from Miyake-jima anorthite (Kimata et al. 1993), which suggests that slab sediments on subducting plates had important role for crystallization of these anorthite megacrysts. These past studies indicate that mineral, melt or liquid inclusions in anorthite megacrysts may afford a clue to the formation process of such minerals. We report the analytical results of sulfide inclusions in anorthite megacrysts from Mt. Fubo (one peak of Minami Zao volcanos). Mt. Fubo is located along the volcanic front and the anorthite megacryst occurs in lavas erupted in the Quaternary period. The chemical analyzes of the anorthite megacrysts (host crystal) and sulfide inclusions were carried out using an electron microprobe analyzer with wavelength dispersive X-ray spectroscopy (EMPA-WDS: JEOL JXA-8230) and/or a scanning electron microscope with energy dispersive X-ray spectroscopy (SEM-EDS: J JEOL JXA-8230). The analytical results show that the anorthite megacrysts from Mt. Fubo contain sulfide inclusions that are droplet-shaped and 30 - 50 micrometer in diameter. The chemical compositions of the sulfide inclusions in anorthite megacrysts are heterogeneous; Fe-rich phase and Cu-rich phase were observed within a single inclusion. Quantitative analyzes suggest that the Fe-rich phase is pyrrhotite [$\text{Fe}_{(1-x)}\text{S}$ ($x=0-0.17$)] and Cu-rich phase is cubanite (CuFe_2S_3), respectively, and these phases contain both Ni and Cu. These sulfide inclusions consisting the two phases may be trapped as fluid inclusions in the host crystals (anorthite megacrysts) at high temperature. The trapped sulfide liquids seem to be separated from silicate melts as monosulfide solid solution ($\text{Fe}_{(1-x)}\text{S}$ - $\text{Ni}_{(1-x)}\text{S}$: Naldrett et al. 1967) or intermediate solid solution (CuFeS_2 : Fleet 2006) and exsolved into pyrrhotite and cubanite in the host crystals upon cooling. The present study indicates that sulfide melts rich in Fe, Cu and Ni were generated within magmas along the volcanic front in Japan.

Keywords: Anorthite, Arc magma, Sulfide, Inclusion

Texture and formation process of jasper, "Nishiki-ishi" from Tsugaru region, Japan

ISHIKAWA, Shiori^{1*}; NAGASE, Toshiro²; KURIBAYASHI, Takahiro¹

¹Institute of Mineralogy, Petrology and Economic Geology, Graduate School of Science, Tohoku University, ²The Tohoku University Museum

Jasper with bright red, yellow and green colors occurs from Tsugaru region, Aomori prefecture, Japan, and is called as "Nishiki-ishi" from its coloring. The jasper is used for ornaments at the region. The colors originate from iron-containing minerals within the jasper. Most raw stones of Nishiki-ishi are usually collected from shingle at beach, and few outcrop of the jasper is found out. Therefore, the occurrence of Nishiki-ishi has not been reported in detail. To elucidate the formation process of Nishiki-ishi, we observed textures of rocks and minerals, and analyzed the chemical compositions of minerals.

Used samples were collected from two localities: Aoiwa, Nakadomari-machi, Kita-tsugaru, Aomori prefecture, and Tappizaki, Sotogahama, Higashi-tsugaru, Aomori prefecture, Japan. Both localities are located in the green-tuff regions of Miocene, and are underlain by pyroxene andesite rocks (Tappi andesite) with volcanic breccia. Silica veins of quartz, chalcedony and opal are locally developed within the rock. Nishiki-ishi mainly consists of quartz and iron-containing minerals, and other minor minerals are barite, apatite and ankerite.

The textures of rocks and minerals were observed using an optical microscope and a scanning electron microscope (JEOL, JSM-7001F), and chemical analyses were carried out using an energy dispersive X-ray analyzer (Oxford, INCA system).

Quartz crystals composing Nishiki-ishi exhibit fibrous spherules with 0.1 mm in diameter or aggregations of micro-crystals with 0.05 mm in width. Comparing with chalcedony and agate, Nishiki-ishi has coarser fibers in the quartz spherules and few zonal-band texture. Origin of its colors is caused by iron-containing minerals; hematite (red), celadonite (green), goethite (yellow), siderite (yellow), pyrite (brown). These iron-containing minerals, which exhibit needle-like or granular forms, are included as fine grains in quartz spherules and fill in space among the quartz spherules.

The macroscopic structure of Nishiki-ishi is a breccia-like or clastic. The breccia fragments consist of aggregates of micro-quartz and optically length-slow types spherules. In contrast, the space among these breccia fragments is filled by clearly euhedral quartz crystals and chalcedony with optically length-fast. These are considerable differences of quartz textures between breccia and the space among of breccia fragments. The original rock of Nishiki-ishi was formed by silicification of volcanic rocks during volcanic activity. After the silicified rocks brecciated, quartz and chalcedony precipitates in the breccia.

Keywords: jasper, Nishiki-ishi, chalcedony, texture

New occurrence and mineralogical properties of rhabdophane group minerals from Higashimatsuura basalt, Kyushu, Japan

UEHARA, Seiichiro^{1*}; SHOBU, Ayaka¹; TAKAI, Yasuhiro²; SHIROSE, Yohei¹

¹Dep. Earth & Planet. Sci. Kyushu Univ., ²Enecom Co., Ltd.

1. Introduction

Higashimatsuura basalt is the alkali olivine basalt distributed in the northwest of Saga Prefecture, Japan. Many rare earth minerals including five new rare earth minerals, kimuraite-(Y) (Nagashima et al., 1986), kozoite-(Nd) (Miyawaki et al., 2000), kozoite-(La) (Miyawaki et al., 2003), hizenite-(Y) (Takai and Uehara, 2013) rhabdophane-(Y) (Takai and Uehara, 2012), were found in the basalts. It is very rare locality that rare earth minerals are found in basalts.

Rhabdophane, (REE) PO₄ • H₂O (REE = La, Ce, Nd, Y), is a hydrous rare earth phosphate mineral. Rhabdophane commonly occurs as a secondary mineral replacing monazite in syenite, alkali syenite pegmatite and sedimentary rock. Recently, many synthetic studies of rhabdophane group minerals are reported for industrial application (e.g., Mesbah et al., 2014). Some rhabdophane which do not found in nature are also synthesized; rhabdophane-(REE) (REE = La, Ce, Pr, Nd, Sm, Gd, Tb, Dy, Y, Er, Yb, Lu) are made (Hikichi et al., 1989; Min et al., 2000). However, detailed occurrence studies of rhabdophane in the nature have not been well investigated.

Takai and Uehara (2012) reported rhabdophane-(Y) as a new mineral from Hinodematsu located in the center of Higashimatsuura peninsula. However, its detailed occurrence of rhabdophane species and their chemical variations were not reported. This paper reports the occurrence, distribution and mineralogical features of rhabdophane group minerals from Hinodematsu and their distribution in Higashimatsuura peninsula.

2. Analysis method

Nineteen samples (H01-H19) were collected from the Higashimatsuura basalt in Hinodematsu. All samples were prepared as several thin sections, and the existence of rare earth minerals were investigated and carried out chemical analyses by scanning electron microscope with EDS (JEOL JSM-5800LV SEM-EDS and JEOL JEM7001F FE-SEM). In some samples, mineralogical features of rare earth phosphates were investigated by SEM (JEOL JSM7001F and Carl Zeiss GEMINI URTRA55 FE-SEM), X-ray diffraction (Rigaku RINT RAPIDII) and scanning/transmission electron microscope (JEM-ARM 200F TEM/STEM).

3. Result and Discussion

(1) Rare earth phosphates from Hinodematsu

Rhabdophane group minerals are found in cavities of the basalts as two types of occurrence at Hinodematsu (Fig.). One is spherical type which is an isolated relatively large spherical (or radiated) crystal with more than 50 μm in diameter composed of very small rhabdophane hexagonal prismatic crystals of few hundreds nm in width. The other is coating type which is aggregated spherical crystals, the size of each spherical crystal is relatively small with one to 10 μm in diameter. Five rare earth phosphates were observed in these two types of spherulites; rhabdophane-(La), rhabdophane-(Nd), rhabdophane-(Ce), rhabdophane-(Y) and xenotime-(Y) like mineral. Chemical compositions of rhabdophane vary widely in one sample. The Nd/La ratios of rhabdophane were constant in one sample and the amount of Y was different. The Nd/La ratios in all samples were divisible into two types, which is Nd-rich type and La-rich type. Rare earth phosphates from Hinodematsu often occur with chemical zoning as coating type and spherical type. In zoning structure, Nd-rich type occurs as spherical type and La-rich type occurs as coating type. Hinodemastu was unique area where many species of rhabdophane group minerals with chemical zoning are found in the alkali olivine basalts.

(2) Rhabdophane group minerals from Higashimatsuura peninsula

Rhabdophanes from Higashimatsuura peninsula are found in several localities and have wide chemical composition as same as the variation found in the Hinodematu rhabdophane group minerals. Rhabdophane-(Ce) is also found. Therefore, rhabdophane group minerals from Hinodematsu and Higashimatsuura peninsula should be primary minerals formed by late stage, low temperature hydrothermal mineral in REE rich alkali basalts.

Keywords: rhabdophane group minerals, rhabdophane-(Y), hydrous rare earth phosphate mineral, Higashimatsuura basalt, Hinodematu

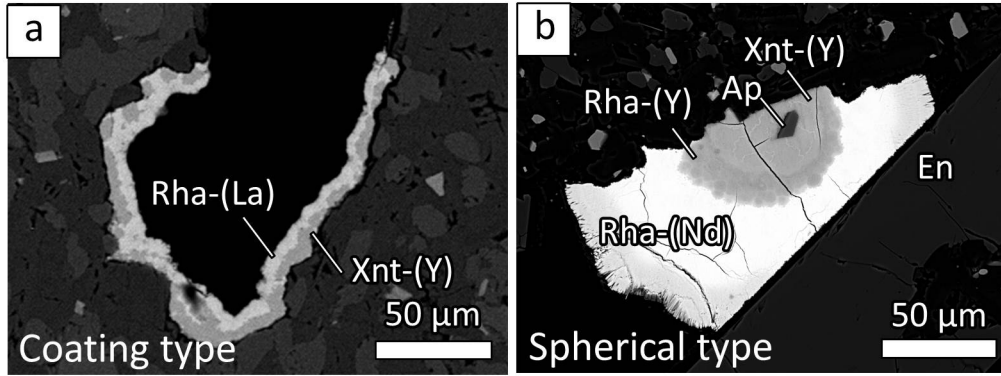


Fig. BSE images of REE phosphates with chemical zoning structure. (a) Cavity coated with rhabdophane-(La) and xenotime-(Y) like minerals (sample H06). (b) Sphere of REE phosphates with zoning structure consisted of rhabdophane-(Nd), rhabdophane-(Y) and xenotime-(Y) like mineral (sample H07).

X-ray CT and Raman spectroscopy analyses of polyphase fluid inclusions of quartz crystals from Tsushima granite

FUJIMOTO, Kyouzuke¹ ; MIYAKE, Akira^{1*} ; TSUCHIYAMA, Akira¹ ; NAKANO, Tsukasa² ; UESUGI, Kentaro³ ; YOSHIDA, Kenta¹ ; MATSUNO, Junya¹ ; KUROSAWA, Masanori⁴

¹Kyoto Univ., ²AIST, ³JASRI, ⁴Tsukuba Univ.

Tsushima granite and the related rocks, southwestern Japan, are known for abundant aqueous polyphase inclusions with large daughter crystals of halite, sylvite, and carbonate. Kurosawa et al. (2012) analyzed chemical compositions of the polyphase fluid inclusions in quartz from miarolitic cavities at Tsushima granite with particle-induced X-ray emission (PIXE), and Kurosawa (2014) directly observed and analyzed the daughter minerals denuded by fracturing the quartz host by using SEM-EDS and identified the phase with Raman microspectroscopy. However, the three dimensional distribution and the morphology of daughter minerals, and the volumes of solid, liquid and vapor phases could not be revealed. Furthermore, it has the potential to transit for daughter mineral to another phase because of the dehydration and so on at fracturing the host to open the inclusion. On the other hand, X-ray computed tomography (XCT) method is the non-destructive analysis and provides the various three dimensional information such as the morphology and the volume. Recently, a linear attenuation coefficient (LAC), which depends on mass density, chemical composition and incident X-ray energy, can be calculated by the synchrotron radiation XCT (SR-XCT) and mineral phase can be inferred from the LAC value. In the present study, we analyzed the polyphase fluid inclusions in quartz crystals from a miarolitic cavity at the Tsushima granite with SR-XCT, Raman microspectroscopy, and SEM-EDS to identify the daughter mineral phases and estimate the chemical composition of daughter minerals and the liquid phases and volume ratios of solid, liquid and vapor phases.

Results from SR-XCT and Raman spectroscopy of two polyphase-inclusion samples, 1A and 1B, show presence of daughter crystals of halite, sylvite, saltonseaitite (K₃NaMnCl₆) siderite, and Fe-OH mineral (goethite?) in the inclusions. The crystals of saltonseaitite, siderite, and Fe-OH mineral, were not reported by the previous SEM-EDS observations (Kurosawa, 2014). Saltonseaitite was first reported by Kampf et al. (2013) and was first observed in Japan. In addition, crystals of calcite and Fe-Cl mineral reported by Kurosawa (2014) could not be observed in this study. The calculated LAC from liquid phase value has the larger value than that calculated from the saturated solution of NaCl or KCl. Thus, it needs to add about 8 mol% Fe to saturated solution of NaCl. We also estimated the volume ratios of the solid, liquid and vapor phases and the bulk chemical composition of each sample. The ratio of vapor to whole inclusion had different values between two neighboring polyphase-inclusions, although the ratios of solid and liquid phases and bulk chemical composition were almost same. This suggests the possibility that these inclusions had been captured at the different period, because fluid inclusions formed at the same generation have usually almost the same volume ratios among vapor and liquid phases. Furthermore, we dug in the quartz to directly observe and analyze the daughter phase in other polyphase-inclusion sample using focused ion beam. Daughter crystals of hematite and unknown phases, which could not be detected in XCT samples, were observed. Because there is a possibility of transiting from Fe-OH mineral observed by XCT and Raman spectroscopy to hematite in vacuum condition.

Kurosawa et al. (2012) 2012 Annual meeting Japan Association of Mineralogical Sciences (Japanese), Kurosawa (2014) 2014 Annual meeting Japan Association of Mineralogical Sciences (Japanese), Kampf et al. (2013) *American Mineralogist*, 98, 231.

Keywords: polyphase fluid inclusion, X-ray CT, Raman spectroscopy, phase identification

Re-examination of phase diagram in Enstatite-Ferrosilite system at 1 atm

OHI, Shugo^{1*}

¹Kyoto University, Science

Pyroxene is one of the most important rock-forming minerals not only for its abundant occurrence but also for various paragenesis which provide information on the thermal history of pyroxene-bearing rocks. In the system $Mg_2Si_2O_6$ - $CaMgSi_2O_6$, there had been the controversy about the appearance and stability of the orthopyroxene (Opx) phase near 1400 C other than protopyroxene (Ppx) since the discovery by Foster and Lin (1975). In recent years, Ohi et al. (2008) observed the isosymmetric phase transition between low-temperature Opx (LT-Opx) and high-temperature Opx (HT-Opx) at 1170 C by high-temperature X-ray powder diffraction (HT-XRD) experiments. They concluded that Opx the phase near 1400 C was HT-Opx. In $Mg_2Si_2O_6$ - $Fe_2Si_2O_6$ system, there was no report about the stability field of HT-Opx. The purpose in present study is to clear the stability field of HT-Opx.

In present study (i) synthetic experiments with gels in $Mg_2Si_2O_6$ - $Fe_2Si_2O_6$ system and (ii) those with Opx crystals were carried out. (i) 28 samples were synthesized from gels with 10 kinds of compositions in $Mg_2Si_2O_6$ - $Fe_2Si_2O_6$ system at temperatures between 1210-1450 C. (ii) Natural Opx (En86Fs14; Bamble, Norway), natural Opx (En83Fs17; Morogoro, Tanzania), natural Opx (En63Fs37; Tamagawa, Ibaragi) and synthetic Opx (En80Fs20 and En70Fs30) was kept at temperatures between 1210-1230 C to observe the transition from Opx to Cpx. Samples of experiments (i) and (ii) were synthesized in one-atmosphere gas mixing (H_2 - CO_2) furnace. The furnace oxygen fugacity maintained near iron-wustite buffer. Recovered samples were analyzed with X-ray powder diffractometer (XRD; Rigaku Smart Lab), a scanning electron microscope (SEM; HITACHI S-3000) and energy dispersive X-ray spectrometer (EDX; HORIBA EMAX7000).

In synthetic experiments of (i), Ppx crystals were observed when En95-85Fs5-15 starting materials were kept at the temperatures 1375-1445 C. Opx phase appeared near 1400 C and En75Fs25 chemical compositions. Cpx phase appeared at temperature between 1200-1300 C. The appearances of Ppx and Opx were coincident with the phase diagram of $Mg_2Si_2O_6$ - $Fe_2Si_2O_6$ system indicated by Huebner (1980), whereas those of Cpx were not. In synthetic experiments of (ii), the phase transition from Opx to Ppx was observed in the run with Natural Opx (En86Fs14) and those from Opx to Cpx were with natural Opx (En63Fs37) and synthetic Opx (En80Fs20 and En70Fs30) at about 1200 C. The transitions showed the stability field of Opx indicated by Huebner (1980) at about 1200 C was incorrect.

The synthetic experiments showed Ppx or Cpx were stable at about 1200 C. Huebner (1980) indicated that there was series of Opx stability field at 900-1400 C because Opx was known as stable phase below 1000 C and Huebner and Turnock (1980) showed Opx was stable around 1400 C. However, Opx below 1000 C was LT-Opx and that around 1400 C was HT-Opx. Therefore, there was no reason to consider the series of Opx stability field at 900-1400 C.

In present study, new phase diagram of $Mg_2Si_2O_6$ - $Fe_2Si_2O_6$ system was proposed in consideration of stability field of below 1000 C and around 1400 C and those of Ppx and Cpx at about 1200 C.

Keywords: orthopyroxene, phase diagram, $Mg_2Si_2O_6$ - $Fe_2Si_2O_6$ system, phase relationship

Origin of siderite-rich rocks from the Ishikari coalfields of Central Hokkaido, Japan(III)

ASANO, Yuki^{1*}; MORIKIYO, Toshiro²

¹Department of Geology, Graduate School of Science Shinsyu University, ²Department of Geology, Faculty of Science Shinsyu University

Ikegami (1958) described mineralogical features of siderite-rich rocks in the Ishikari coalfield at first time. After that, origin of these characteristic rocks were investigated by Matsumoto and Iijima (1981). Asano et al. (2014) measured whole-rock chemical compositions and carbon-oxygen isotope ratios of sideritic rocks, which had not been reported to that time. They reached a new view as to the genesis of siderite, which is different from Matsumoto and Iijima (1981). Subsequently, Asano and Morikiyo (2015) studied Mn/Fe ratios and carbon-oxygen isotope ratios of calcite and siderite in the rocks. On the basis of the chemical data and textural observation, they conclude that crystallization of calcite occurred before the precipitation of siderite. Calcite precipitation is due to the reduction of $\text{Fe}(\text{OH})_3$ by carbonaceous matter, which is abundant in the coaly bed.

In this poster presentation, we describe the entire process of sideritic rock formation in the Ishikari coal field.

1. The source of iron of siderite is thought to be dissolved Fe^{2+} in stream water. The water flows into the lake of meandering river area of plains. Then the water becomes exposed to the oxygen-rich atmosphere. This lead oxidation of dissolved Fe^{2+} and Mn^{2+} to $\text{Fe}(\text{OH})_3$ and $\text{MnO}_2 \cdot n\text{H}_2\text{O}$. These solid particles of hydro-oxides were deposited at the bottom of the lake together with FePO_4 .

2. Most of $\text{Fe}(\text{OH})_3$ was contained in the clastic materials with a dispersed fashion. But in some cases, they accumulate at the bottom of a lake horizontally forming thin layers of iron-rich sediments. The chemical compositions of the host clastic matter is similar to the average shale.

3. With the progress of sediment burial, sediments-pore water system became anoxic. Then, $\text{Fe}(\text{OH})_3$ deposited within the sediments were reduced to be Fe^{2+} by the reaction with carbonaceous matter, which was abundant in the sediments. Production of CO_2 by the oxidation of carbonaceous matter brought in the precipitation of calcite of low $\delta^{13}\text{C}$ value. At the time of decreasing in Eh, $\text{MnO}_2 \cdot n\text{H}_2\text{O}$ is reduced prior to $\text{Fe}(\text{OH})_3$ reduction. Because of this, the Mn/Fe ratio of calcite is higher than that of siderite. 4. Since the concentration of SO_4^{2-} ion of river water is low, the sulfate reduction ceased in an early stage of diagenesis. Then the methane fermentation begins. At this stage, the siderite possessing positive, high $\delta^{13}\text{C}$ value started to precipitate forming the siderite nodules and thin beds of sideritic rocks.

- Asano, Y., Kusakabe, T., and Morikiyo, T. (2014) Formation of sideritic rocks in the Ishikari coalfield — particularly on the source and precipitation of iron. The 121st Annual Meeting of the Geological Society of Japan Abstracts R9-O-4, p.96
- Asano, Y. & Morikiyo, T. (2015) Formation processes of sideritic rocks in Central Hokkaido Ishikari coalfield (II) — For Calcite coexisting with Siderite. The Annual Meeting of the Sedimentological Society of Japan Abstracts. (Submitted to.)
- Ikegami, S (1958) Preliminary Note on the Sideritic Band (Ironstone) in the Horokabetsu Formation in the ishikari Coal Field., Mineralogical Journal, volume3, No.6, 592-596
- Matsumoto, R. and Iijima, A. (1981) Origin and diagenetic evolution of Ca-Mg-Fe carbonates in some coalfield of Japan. Sedimentology, 28, 239-259.

Keywords: carbonate concretions, behavior of the elements, Ishikari coalfield

REE and Sr and Nd isotopic compositions of granitic rocks from the Hua Hin area, Thailand

YUHARA, Masaki^{1*}; KAMEI, Atsushi²; NAKANO, Nobuhiko³; YOSHIMOTO, Aya³; KAWAKAMI, Tetsuo⁴; KAMIKUBO, Hiroshi⁵; OSANAI, Yashuhito³; CHARUSIRI, Punya⁶

¹Fukuoka Univ., ²Simane Univ., ³Kyushu Univ., ⁴Kyoto Univ., ⁵JOGMEC, ⁶Chulalongkorn Univ.

The granitic rocks are widely distributed in the Hua Hin area, Thailand. This area is located in the Central Province (Cobbing, 2011) consists mainly of S-type granitic rocks, whose ages range from early Late Triassic to late Early Jurassic (ca. 230-180 Ma) (Sone and Metcalfe, 2008). The petrogenesis of these granitic rocks is explained by partial melting of the Sibumasu crust subducted beneath the Palaeo-Tethys accretionary complex (Sone and Metcalfe, 2008). However, characteristic of source material of granitic rocks in the Hua Hin area are poorly understood. In this paper, we report REE and Sr and Nd isotopic compositions of granitic rocks from this area.

The granitic rocks in the Hua Hin area are composed of foliated granitic rocks and non-foliated granitic rocks. The formers are the Hub Kapong Gneissic Granite, Hua Hin Gneissic Granite and Pran Buri Gneissic Granite. The Hub Kapong and Hua Hin Gneissic Granites are partly weakly mylonitized K-feldspar porphyritic biotite granite. The Hub Kapong and Hua Hin Gneissic Granites give Rb-Sr whole-rock isochron ages of 202 \pm 22Ma and 209 \pm 14Ma, respectively (Yuhara et al., 2011). Kawakami et al. (2014) reported 219 \pm 2Ma and 185 \pm 2Ma U-Pb zircon ages from the Hua Hin Gneissic Granite, and interpreted that these ages represented the timing zircon crystallization and regional metamorphism of upper amphibolite facies grade, respectively. The Pran Buri Gneissic Granite is mylonitic biotite granite. Non-foliated granitic rocks are stock bodies intruded into the Hub Kapong Gneissic Granite, and composed of biotite to two-mica granite. A body of non-foliated granitic rocks gives an Rb-Sr whole-rock isochron ages of 84 \pm 13Ma (Yuhara et al., 2011). These granitic rocks have peraluminous chemical composition (Yoshimoto et al., 2010).

Chondrite-normalized REE patterns of these granites are enriched in light REE (LREE) and depleted in heavy REE (HREE). These granites show Eu anomalies. Non-foliated granitic rocks show flat patterns in HREE. Initial epsilon Sr and Nd values of the Hub Kapong and Hua Hin Gneissic Granites are 270 to 340 and ?15.6 to -8.8, and 240 to 360 and ?13.5 to -9.3, respectively. Model epsilon Sr and Nd values of the Pran Buri Gneissic Granite calculated by 209Ma are 510 to 1040 and ?8.7 to -6.9. Initial epsilon Sr and Nd values of non-foliated granitic rocks are different every bodies, and are 970 and -11.2, 440 and -10.6, 60 and -9.8, respectively.

Keywords: REE composition, Sr and Nd isotopic compositions, granitic rocks, Hua Hin, Thailand

Rare elements concentration related to behavior of the H₂O, F, B and P, in Nagatare pegmatite, Fukuoka Prefecture

SHIROSE, Yohei^{1*} ; ITO, Shin¹ ; UEHARA, Seiichiro¹

¹Dept. Earth & Planet. Sci., Fac. Sci., Kyushu University

Nagatare pegmatite, located at the western area of Fukuoka City, Fukuoka Prefecture, is considered that it derived from the Sawara granite, which intruded into the Itoshima granodiorite (Karakida et al., 1994). The pegmatite also intruded into the Sangun metamorphic rocks. The most characteristic properties of Nagatare pegmatite is the enrichment of rare elements such as Li, Cs and Ta, resulting as the occurrence of various rare element minerals. We have been investigating about each mineral in detail (e.g., Shirose and Uehara, 2014). There are differences for each dyke on constituent minerals and internal textures. Li enriched pegmatite is only one dyke located in Mt. Nagatare, and many of the dykes are simple pegmatites, bearing a common granite composition. In this study, the variation of constituent minerals, and chemical compositions of accessory minerals were studied, and the forming process of Li pegmatite were discussed with a focus on H₂O, F, B and P as flux components in granite melts.

Li mineral deficient pegmatites often occurred with aplites, with a dyke-shape body, 5-20 m in width and elongating along N20°W, which is concordant with lamination structures of Sawara granite. The pegmatites were mainly consisted of quartz, K-feldspar, albite and muscovite, showing simple pegmatite compositions close to the chemical composition of granite. However, some pegmatites contained rare elements minerals such as beryl and columbite, without Li minerals, indicating the concentrations of rare elements including Be, Nb and Ta. In addition, they contained garnet and gahnite, indicating the peraluminous compositions. A pegmatite dyke intruding metamorphic rocks had tourmaline as borosilicate mineral, in addition to garnet and beryl. In Li pegmatite, in addition to the minerals above, triplite and montebrasite-amblygonite occurred as fluorine phosphates, and abundant lepidolite existed as F enriched mica.

As for chemical compositions of tourmaline, Fe and Mg were dominant without F contents in the tourmaline from the pegmatite intruding metamorphic rocks, while the tourmaline from Li pegmatite show fractionated trends from Fe-Li to Li-Al dominant chemical compositions with F enrichment. F contents of montebrasite-amblygonite show a high F concentration at the central part of Li pegmatite, 1.4-2.0 wt% F contents, using the partition coefficient to melt estimated by London et al. (2001). Columbite group minerals [(Fe, Mn)(Nb, Ta)₂O₆] were common accessory minerals in the Nagatare pegmatite. The chemical trends are Mn/(Mn+Fe) = 0.3-0.6 with Nb enrichment in the simple pegmatites, and Mn/(Mn+Fe) = 0.4-1.0 with Nb to Ta enrichment on Mn endmember. Their chemical trends coincide with that of columbite group minerals, suggested by Wise et al. (2012), corresponding to F contents of pegmatite.

In Li pegmatite from Nagatare, primary Li-tourmaline and K-feldspar had undergone alteration to clay minerals such as muscovite and cookeite. Montebrasite-amblygonite also altered into various secondary phosphates and muscovite. These reactions are hydrothermal replacement by H₂O enriched residual fluids in the late stages of pegmatite forming process, and it is suggested as a characteristic reaction in the H₂O enriched Li pegmatite. On assuming the latest elemental behavior, it is required to reveal these alteration processes and behaviors of B and Li released by tourmaline breakdown.

It is assumed that chemical and zonal developments of pegmatite are highly controlled by flux components in granite melts such as H₂O, F, B and P. As for Nagatare Li pegmatite, it is characterized by enrichment of F contents. In many cases, these elements are derived from peraluminous granite, considered to melt matasedimentary rocks, and we need to focus on properties of the surrounding granite, in addition to P-T conditions of formations.

Keywords: Li pegmatite, Nagatare, rare elements, tourmaline, fluorine, flux

Rare earth element compositions of Neogene plutonic rocks, North Fossa Magna, Japan

KAWANO, Yoshinobu^{1*}

¹Department of Environment Systems, Faculty of Geo-environmental Science, Rissho University

Neogene plutonic rocks are distributed in North Fossa Magna (NFM), and consist of mainly quartz diorite. Chino, Shimosuwa, Wada, Matsumoto, Utsukushigahara and Yori bodies, Ueda, Horikiri and Myoutoku-Yonago bodies and Makihatayama, Tanigawadake and Akayu bodies expose in Utsukushigahara-Kirigamine (UK), Suzaka-Ueda (SU) and Makihata-Tanigawa (MT) areas, respectively. It is considered that these plutonic rocks in NFM are derived from upper mantle, since they are characterized by low K_2O/Na_2O ratio and Tin content (Ishihara et al., 1976).

In chondrite normalized REE patterns, the Chino and Shimosuwa bodies in UK area have weak negative Eu anomalies, whereas others in same area show no anomalies. The Matsumoto, Wada and Chino bodies are characterized by LREE enrichment. All bodies in UK area have relatively constant patterns of HREE, but the Wada body has low HREE contents. The Myoutoku-Yonago body in SU area has weak negative Eu anomaly, and is characterized by LREE enrichment. All bodies in SU area have also relatively constant patterns of HREE. The Makihatayama and Tanigawadake bodies in MT area have negative Eu anomalies, and show right downward sloping patterns of LREE and constant patterns of HREE. La/Sm_N and La/Yb_N ratios of all bodies in three areas increase with decreasing SiO_2 contents. It suggested that LREE concentrated to residual magma and change of HREE was small. Eu/Eu^* ratio of those slightly decreases with decreasing SiO_2 contents, and the rocks in UK area have higher ratios of Eu/Eu^* than those of SU and MT areas.

The plutonic rocks distributed in respective areas have peculiar features of REE, suggesting that they have different origin and magma process.

Keywords: North Fossa Magna, Neogene, plutonic rock, rare earth element

Origin of the Miocene mafic volcanic rocks distributed in Utsunomiya and Kanuma, central Japan

SHIMIZU, Ryuichi^{1*} ; KAWANO, Yoshinobu²

¹Graduate School of Geo-environmental Science, Rissho University, ²Faculty of Geo-environmental Science, Rissho University

Two types of volcanic rocks were reported from Miocene formation distributed in Utsunomiya area, central Japan. Andesite and rhyolite are intercalated with the Kazamiyamada Formation, in the lower, and the Oya Formation, in the upper, respectively. The Kazamiyamada formation derives subaerial volcanism, and in contrasts the Oya formation formed by submarine volcanic eruption. K-Ar whole rock ages of the Kazamiyamada andesite and the Oya rhyolite are reported as 14.8-16.6 Ma and 14.2 Ma, respectively (Yoshikawa, 1998; Yoshikawa et al., 2001). These ages of igneous activity correspond to the opening event of Japan Sea. The authors reported chemical characteristics of volcanic rocks occurred in the Utsunomiya area (Shimizu and Kawano, 2013).

On the other hand, Miocene Primitive Basalt, Andesite and Dasite distributed are Kanuma area from Hinata formation, to the west side of the Utsunomiya area.

This study compared the Kazamiyamada andesites with the Hinata mafic volcanic rocks.

Keywords: Miocene volcanism, Utsunomiya area, Kanuma area, Sr and Nd isotope ratios

Establishment of new index of sediment input into granitic magma using trace element composition in zircon

SUZUKI, Kazue^{1*} ; SAWAKI, Yusuke¹ ; HATTORI, Kentaro² ; HIRATA, Takafumi² ; ARAI, Hiroyoshi³ ; OMORI, Soichi⁴ ; MARUYAMA, Shigenori⁵

¹Department of Earth and Planetary Sciences, Tokyo Institute of Technology, ²Division of Earth and Planetary Sciences, Kyoto University, ³Waseda University Honjo Senior High School, ⁴The Open University of Japan, ⁵Earth-Life Science Institute, Tokyo Institute of Technology

Understanding of formation process of granitic magma is one of the important issues to unveil evolution of Earth history. Evaluating amounts of sediment incorporation into granitic rocks is necessary to comprehend formation process of granite. Sedimentary components in granite have been estimated from whole rock geochemistry such as alumina saturation index and radiogenic Sr isotopic ratio. However, these whole-rock values do not necessarily reflect original magma composition, because chemical composition of the magma changes with magma evolution process (e.g. Griffin et al., 2002; Belousova et al., 2006).

Trace element compositions in zircon could be a useful tracer for evaluating amounts of sediment contamination into granitic magma (e.g. Belousova et al., 2006). In order to establish a new indicator for estimating quantity of sedimentary components in granite, we focus on modern granitic belts where tectonic settings are well constrained. We conducted in-situ analyses of trace element compositions in 188 zircon grains from the Tanzawa Tonalite (4-9 Ma; Tani et al., 2010) and 210 zircon grains from the Taitao Granitoid (4-5 Ma; Anma et al., 2009) with LA-ICP-MS. The Tanzawa Tonalite is the best target for this study, because it emplaced at middle crust of immature oceanic island arc where influence of sedimentary contamination is extremely low. On the other hand, the Taitao Granitoids contain small amount of sedimentary components because the granitoid were intruded into Jurassic accretionary complex.

Zircons from the Tanzawa Tonalite and the Taitao Granitoid show enrichment of HREE, negative Eu anomaly and positive Ce anomaly, which are typical characteristics of those in most granites. Trace element compositions in zircons from the Taitao Granitoids show lower Yb/Sm ratios than those from the Tanzawa Tonalite. As combined with previous trace element data in zircons from oceanic plagiogranite, S-type granite and I-type granite, a clear correlation can be observed between $\ln(\text{Ce}/\text{Ce}^*)$ and $\ln(\text{Yb}/\text{Sm})$. Higher Ce/Ce* and Yb/Sm ratios in the Tanzawa Tonalite are consistent with little sedimentary component deduced from its tectonic setting. In addition, results from principal component analysis using these trace element data show strong correlations among $\ln(\text{La}/\text{Sm})$, $\ln(\text{Pr}/\text{Sm})$ and $\ln(\text{Nd}/\text{Sm})$ values in zircons. Cross-plots of these values exhibit that trace element compositions in zircons from the Tanzawa Tonalite and oceanic plagiogranite are plotted on different fields from those from S-type granites. High La/Sm, Pr/Sm and Nd/Sm ratios in zircons from the S-type granite probably reflect high LREE concentration in sediments. Therefore, these trace element compositions can be useful to evaluate influence of sedimentary components into granite. The results in this study demonstrate that trace element composition in zircons has a possibility to provide more detail information for protolith of granite.

Keywords: Zircon, Trace element composition, LA-ICP-MS, Tanzawa Tonalite, Taitao Granite, Sediment contamination

Serpentinite and Rodingite from Mikabu belt, Central Japan

ENJU, Satomi^{1*} ; UEHARA, Seiichiro¹

¹Department of Earth and Planetary Sciences, Faculty of Sciences, Kyushu University

Introduction

Serpentinites are valuable evidence of hydrothermal activity in deep earth. They are often made by hydrothermal alteration of peridotite, the main component of the mantle, at relatively low temperatures. They form in specific conditions, such as subduction zone and mid-atlantic ridges. They capture and release various elements during formation, playing an important role in the geochemical cycles and biological activity (Fruh-Green, 2004).

Rodingites are greatly affected by fluid of serpentinization. Rodingites are Ca-rich, Si-poor rocks often seen at serpentinite outcrops, composed by diopside clinocllore and various Ca-Al silicates. It is thought to form by hydrothermal alteration by the fluid, who experienced serpentinization (e.g. Coleman, 1967; O' Hanley et al., 1992). The mineral assemblage seems to be affected by the composition of the fluid, showing various combinations within the same locality, though the system is not totally understood (Kobayashi and Shoji, 1988; Li et al., 2007).

Methods

In this study the formation process of serpentinite and rodingite was investigated by the observation of the samples from ultramafic body in the Mikabu green rocks, central Japan. The samples were collected from Nakauri and Yoshikawa in Aichi prefecture, and Shiokawa peridotite body in Nagano prefecture (Makimoto, 1978; Uesugi and Arai, 1999). In this presentation, the samples from Shiokawa peridotite were mainly handled. The constituent minerals were determined by X-ray diffraction pattern, and texture observation and quantitative chemical analysis was carried out by scanning electron microscope.

Results and Discussion

The main contents were dunite and serpentine with various degree of serpentinization. The serpentinized part often included clinopyroxene, showing that wehrlite altered to serpentinite while dunite remained fresh. Rodingite was seen as dikes of few meters or of few centimeters in size, accompanied by dunite or serpentinite. The consistent minerals were diopside, clinocllore, vesuvianite, and andradite.

In serpentinite, an Al-rich area of serpentine, which seem to take shape of the primary mineral, was often seen. In one sample, pumpellyite-(Al) and grossular was seen in the center of this texture, formed by the saussurization of plagioclase. A needle like clinopyroxene, Ca-poor than the primary clinopyroxene, was seen around this structure, and the following formation sequence is proposed. First, the plagioclase undergoes saussuritization and turns into fine grained minerals such as pumpellyite-(Al), grossular. Then those minerals become Al-rich serpentine and releases Ca, forming clinopyroxene of needle like shape, replacing the surrounding olivine and evolving around the primary clinopyroxene with sharp contacts. Needle like clinopyroxenes were seen where the degree of serpentinization is high, indicating that this reaction caused by plagioclase accelerates serpentinization.

In rodingite, a primary clinopyroxene, showing the same features as those in serpentinite, was replaced by vesuvianite, andradite, clinopyroxene. The estimated order of formation is diopside, vesuvianite, andradite, Fe-rich andradite, and clinocllore were present in all stages. The mineral of the host rock is thought to be clinopyroxene and saussurized plagioclase. Therefore, the rodingite veins should have formed in the gabbrotic part of the peridotite, which means the source and receiver of rodingitization coexists inside a single rock type.

As mentioned above, rodingite coexists with dunite in this locality, which is quite unique, since most reported rodingites accompanies completely serpentinized serpentinite. Rodingite of this occurrence lack the soure of the serpentinized fluid, so the transportation is essential for formation. Since the rodingites show the same features irrelevant to the degree of serpentinization of the surrounding rock, the same fluid was thought to be supplied from the surrounding serpentinites.

Keywords: serpentinite, rodingite, dunite, needle like clinopyroxene, serpentine, clinocllore

U-Pb zircon dating of the Late Cretaceous volcanic rocks from the Ikuno and Mitsuishi mines area, southwest Japan

SATO, Daisuke^{1*}

¹GSI, AIST

Numerous hydrothermal ore deposits occurred in Late Cretaceous to Paleogene igneous rocks are distributed in the Inner Zone of southwest Japan. The Ikuno mine in north-central Hyogo Prefecture is hydrothermal polymetallic ore deposit. This mine was produced by replacement of the Late Cretaceous dacite to rhyolite tuff and lapilli tuff of the medium to lower Ikuno Formation and dikes by high temperature fluids probably generated around granitic rocks. The Mitsuishi mine in southeastern Okayama Prefecture is hydrothermal pyrophyllite and sericite deposit. This mine was produced by replacement of the Late Cretaceous rhyolite welded tuff and lapilli tuff of the lower Wake Formation by high temperature fluids.

U-Pb zircon dating using LA-ICP-MS was carried out for 2 pyroclastic flow deposit samples from the Late Cretaceous volcanic rocks in the Ikuno and Mitsuishi mine area, southwest Japan. The Ikuno and Mitsuishi mines are determined to be 78.9 ± 0.9 Ma and 82.4 ± 0.6 Ma, respectively.

Keywords: U-Pb age, Ikuno mine, polymetallic vein, Mitsuishi mine, pyrophyllite and sericite clay deposit, Late Cretaceous

Geochronology of detrital zircon from the Highland Complex, Sri Lanka: Implications for Gondwana reconstruction

TAKAMURA, Yusuke^{1*}; TSUNOGAE, Toshiaki¹; SANTOSH, M²; MALAVIARACHCHI, Sanjeeva p.k.³; TSUTSUMI, Yukiyasu⁴

¹Faculty of Life and Environmental Sciences (Earth Evolution Sciences), University of Tsukuba, ²School of Earth Science and Resources, China University of Geosciences Beijing, ³Department of Geology, Faculty of Science, University of Peradeniya, ⁴Department of Geology and Paleontology, National Museum of Nature and Science

Sri Lanka is regarded as one of the important regions to unravel the process of Gondwana amalgamation because it was located in the center of the collisional orogeny formed during Late Neoproterozoic. The Highland Complex, exposed at the central part of Sri Lanka, is metamorphosed to granulite-facies conditions (e.g., Faulhaber and Raith, 1991; Hiroi et al., 1994; Raase and Schenk, 1994). Ultrahigh-temperature metamorphic conditions are also reported from some localities in the Highland Complex (e.g., Osanai et al., 2006; Sajeev and Osanai, 2004; Sajeev et al., 2007). The Highland Complex is dominantly composed of metasediments that include detrital zircons, and their age distributions can be used to infer the correlation between some depositional basins and their provenance (e.g., Collins et al., 2007; Kuznetsov et al., 2014). Although some authors (Holzl et al., 1994; Kroner et al., 1987) obtained Archean to Paleoproterozoic detrital zircon ages from metasediments in the Highland Complex, they did not discuss about the detail correlation of the Highland Complex with other Gondwana fragments. This study focuses on geochronology of detrital zircons in metasediments from the Highland Complex in order to unravel the regional geographical correlation of Sri Lanka within Gondwana supercontinent.

We collected four samples of quartzite and pelitic gneiss from the Highland Complex, separated detrital zircons from them, and analyzed U-Pb ratios using LA-ICP-MS. The detrital zircon ages are distributed from ca. 3500 Ma to ca. 1700 Ma with strong peaks at around 2700 Ma, 2500 Ma, and 2000 Ma. These age distributions of detrital zircons are consistent with those from the Palghat-Cauvery Suture Zone (e.g., Raith et al., 2010; Sato et al., 2011), but different from those of the Trivandrum Block and the Achancovil Shear Zone (Collins et al., 2007), South India, because they have Mesoproterozoic detrital age not found in the Highland Complex zircons. Thus, the Highland Complex could be correlated with the Palghat-Cauvery Suture Zone as a sedimentary basin rather than the Trivandrum Block or the Achancovil Shear Zone in southern India.

The precursor of the Wannai Complex could be a possible source of the Highland Complex before it was reworked based on available Hf crustal model ages of zircon (Santosh et al., 2014). The Dharwar Craton (ca. 3400-2500 Ma; Chadwick et al., 2000; Collins et al., 2003), the Salem Block (ca. 2750, 2600, 2500 Ma; e.g., Collins et al., 2014; Ghosh et al., 2004; Saitoh et al., 2011), and northern Madurai Block (ca. 2500 Ma; Collins et al., 2014; Plavsa et al., 2012; Teale et al., 2011) are also possible provenances of sediments of the Highland Complex. In contrast, crustal blocks in East Africa are difficult to be source regions of the Highland Complex because they are composed of rock units younger than Mesoproterozoic (Kibaran belt; ~1400 Ma; Kokonyangi et al., 2004).

Keywords: Gondwana, Sri Lanka, The Highland Complex, Detrital Zircon, LA-ICP-MS, Suture Zone

Metamorphic P-T evolution of garnet-clinopyroxene rocks from the Gondwana collisional orogen in southern India

YANO, Minami^{1*} ; TSUNOGAE, Toshiaki² ; IINUMA, Minako² ; SANTOSH, M³

¹Univ. Tsukuba, ²Univ. Tsukuba, ³China Univ. Geosci.

The East African - Antarctic Orogenic Belt, which includes Madagascar - Southern India - Sri Lanka - East Antarctica regions, is regarded to have been formed by complex subduction-accretion-collision tectonic events related to the amalgamation of Gondwana Supercontinent during Neoproterozoic. The Palghat-Cauvery Suture Zone in southern India is known as a major suture zone that formed during the closure of Mozambique Ocean at ca. 530-550 Ma. The dominant lithologies of the suture zone are felsic to intermediate orthogneiss, metasediments, and mafic-ultramafic suites. Particularly, the occurrence of mafic-ultramafic suites (ophiolite or layered intrusion) is a unique character of the suture zone compared to surrounding granulite blocks and cratons. Here, we report new petrological data of metagabbroic garnet-clinopyroxene rocks from southern India and discuss its petrological implications. Mineral assemblages of the rocks are garnet + clinopyroxene + ilmenite + plagioclase + quartz with retrograde hornblende. Similar rocks and textures have been reported from the Palghat-Cauvery Suture Zone in South India (Nishimiya et al., 2008; Saitoh et al., 2011), Highland Complex in Sri Lanka (Osanai et al., 2006; Takamura et al., 2014), and Lutzow-Holm Complex in East Antarctica (Saitoh et al., 2012). However, temperature and pressure conditions inferred for the metagabbro based on geothermobarometry are 680-710C and ~9 kbar, which is significantly lower than the results of previous studies (>12 kbar, >800C). The metagabbro could be an exotic block with discrete P-T evolution trapped during the formation of the Palghat-Cauvery Suture Zone.

Keywords: granulite, P-T path, Gondwana

Proposal of a portable particle size analyzer by a spatial filter velocimetry for a field work of geoscience.

SATO, Fumiaki^{1*} ; SASAKURA, Daisuke¹

¹Malvern instruments A division of Spectris Co., Ltd.

1.Introduction

The existing popular approach at geoscience to measure particle size analysis is a sieving technique. The sieving has advantages such as portability, robustness and easy to understand. The drawback of the sieving are low resolution to particle size, require of a long period of time to measure and bulky equipment. Therefore, real time analysis, compact equipment, wide range and high resolution methods may be preferable at the recently geoscience research. One of approach to respond to this issue is a inline particle analysis by spatial filter velocimetry (SFV) method. SFV method is one of application of light blocking (obscuration) methodology, and it has capability to wide range particle size measurement such as in micron to centimeter with a several decade second. This approach has capability to investigate sample in nature, such as a cray, sand and a sea soil on anywhere. This report will propose to capability and application to particle size analysis for geoscience by SFV method.

2.System

A Parsum (Malvern Instruments) was proposed to this application. The advantages of this device are compact, lightweight , battery drive is possible and a calibration free. The specification of particle measurement range is 50 to 6,000um which is sufficient to generally geoscience application.

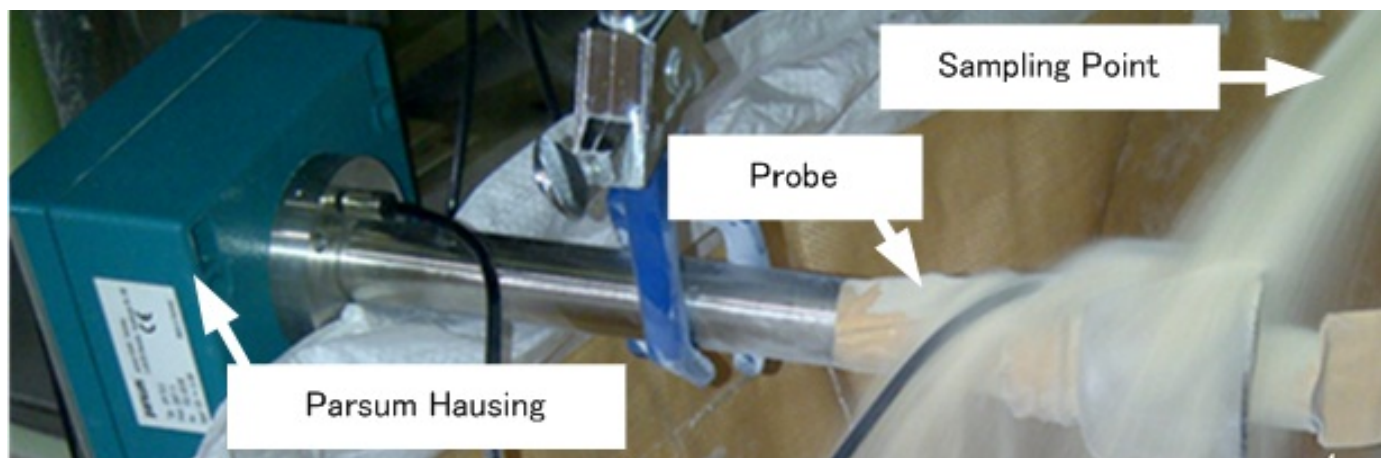
3.Feasibility study

It was shown that schematic picture at feasibility study in Fig.1. This application is real time monitoring powder transportation in the field of certain industry. It was comparable study between the sieving with intermittently sampling and SFV method with real time monitoring. As result of volume fraction in 150um were 64.2% by SFV method and 57.4% by sieving . This meaning is similar result in both methods.

4.Conclusion

This report will propose other applications for field work in this study.

Keywords: Real time inline particle analysis, Portable particle size analyzer, Sieving technique, A field work of geoscience., A spatial filter velocimetry



In-situ observation of formation process of carbon-rich minerals in several sites of Yamaguchi, Japan.

MIURA, Yasunori^{1*}

¹Yamaguchi, Visiting Univ.(In & Out)

1. Characteristics of carbon minerals: Carbon-bearing minerals are significant minerals to show the detailed formation process. Dynamic samples might elucidate new information of micro- to macro-carbon minerals, which are main purposes of the present paper [1-4].

2. Carbon-rich minerals from Yamaguchi Prefecture: Present carbon-bearing samples are used from three sites (Yamaguchi) and one site (Shimane) to compare dynamic formation processes[1-4].

3. Microscopic observation of carbon-containing minerals: Microscopic carbon-bearing minerals are obtained at the following six location-samples as follows [2-4].

1) Point A: Historical sample-site of basalt with phlogopite and feldspar contains microscopic carbon-bearing grains quenched as flake texture found in this study.

2) Points B: Basalt with phlogopite and feldspars shows more detailed grains and texture with tube-shaped texture with progressive change of carbon-contents. The present observation is new result to be found as carbon-separated concentrations during fluid-solid reactions shown as flake quenched texture.

3) Points C: Basalt phlogopite mica and feldspar shows carbon-bearing materials with quenched flake texture and tube-like textures.

4) Points D: Basalt with phlogopite minerals contains carbon-bearing grains with flake and tube-like textures.

5) Point E: Basalts with feldspar minerals (without any phlogopite) shows carbon-bearing grains on feldspar minerals.

6) Points F: Carbon-rich grains can be found separately on feldspar surface (without phlogopite).

4. Identification of carbon minerals: Carbon-rich grains from point B have been investigated by X-ray diffraction and Raman Spectroscopy, where the characteristics of high pressure-type carbon minerals(diamond-like) have been obtained in this study.

5. Formation of high-pressured carbon minerals: Dynamic process and tube-like texture indicate carbon-separation from carbon-bearing minerals during shock wave processes of volcano and impact process.

6. Summary: Carbon-rich grains of high-pressure form (microscopic diamond) are obtained on the Yamaguchi samples (grain B) compared with other samples in Japan, where carbon-separation and concentration can be developed along solidified tube-like and fluid-like process with quenching found in the study.

References: [1] Miura Y. (2007): *Front. Mineral Sci.* (Cambridge Univ.), 223. [2] Miura Y. (2008): *Am. Geo. Union*, pp.1. *EOS Trans, AGU*, 89 (53), MR33-B1861. [3] Miura Y. (2012-2014): *Japan Journal of Geological Society* (Osaka, Tohoku and Kagoshima Universities), pp.1. [4] Miura Y. (2014): *Inter. Mineral. Assoc.* 2014 (Johannesburg, SA), 689.

Keywords: High-pressure carbon, Basalt, In-situ observation, Phlogopite, Fluid solidified, Tube-like texture